Energy exchange and evapotranspiration over irrigated seed maize agroecosystems in a desert-oasis region, northwest China

Yongyong Zhang [a,*], Wenzhi Zhao [a], Jianhua He [b], Kun Zhang [b]

[a] Linze Inland River Basin Research Station, Key Laboratory of Eco-hydrology of Inland River Basin, Cold and Arid Regions Environmental and Engineering Research Institute, Chinese Academy of Sciences, Lanzhou 730000, China
[b] Key Laboratory of Western China's Environmental Systems (Ministry of Education), College of Earth and Environmental Sciences, Lanzhou University, Lanzhou 730000, China

ARTICLE INFO

ABSTRACT

Investigating the dynamics of energy and water vapor exchange in oasis agroecosystems is important to improve scientific understanding of land surface processes in desert-oasis regions. In this study, water vapor and energy fluxes were obtained by using an eddy covariance technique for two similar irrigated seed maize fields at Yingke and Pingchuan, in northwest China. Seasonal variabilities of evapotranspiration (ET) and relevant environmental and biophysical factors were explored. Results showed that the energy balance closures were reasonable, with energy balance ratio of 0.99 and 0.79 for a half-hourly time scale at Yingke and Pingchuan, respectively. The seasonal changes in net radiation (R_n), latent heat flux (LE), and sensible heat flux (H) of Yingke and Pingchuan were similar. Net radiation was 11.27 MJ m^{-1} day^{-1} during the growing season. Latent heat flux accounted for 67.5% of net radiation, sensible heat flux was 25.0%, and soil heat flux was 7.5%. A reverse seasonal change was found in partitioning energy flux into LE and H. The seasonal variation in energy flux partitioning was significantly related to the phenology of maize. During the growing season, ET was 467 and 545 mm, and mean daily ET 2.84 and 3.35 mm day^{-1} at Pingchuan and Yingke, respectively. "Non-growing" season ET was 15% of the annual ET in the bare field (during October–March) and 85% of the annual ET for maize (during April–September). Daily ET was mainly controlled by net radiation and air temperature, and was significantly affected by leaf area index (<3.0 m^2 m^{-2}) and canopy conductance (<10 mm s^{-1}). Furthermore, irrigation promoted daily ET greatly during the growing season. Accurate estimation of seed maize ET and determination the controlling factors helps to develop exact irrigation scheduling and improve water resource use in desert-oasis agroecosystems.

© 2016 Elsevier B.V. All rights reserved.

1. Introduction

Solar radiation provides the basic energy for a variety of physical and biological processes occurring on the Earth's surface (Sen, 2004). Energy and water vapor exchange processes between the land surface and atmosphere drive photosynthesis, evapotranspiration, sensible heat flux, energy storage in vegetation, and heating of the soil (Baldocchi et al., 2000; Gu et al., 2005; Mccaughey et al., 1997). The energy balance in agroecosystems influences regional mass and energy exchange between the surface biosphere and atmosphere, water circulation, and climate changes. Energy flux partitioning is often used to describe the energy balance (Chen et al., 2009; Lei and Yang, 2010). Net radiation is parti-

tioned into sensible, latent, and surface storage heat flux, which are controlled by meteorological factors, biological factors, vegetation condition and phenology, and soil moisture (Baldocchi et al., 2000; Gu et al., 2005; Hao et al., 2007; Wever et al., 2002). The desert-oasis agroecosystems play a crucial role in maintaining the stable ecological environment and agriculture productivity (Zhang and Zhao, 2015b). Understanding the basic characteristics of energy and water vapor exchange in desert-oasis agroecosystems is important for modeling crop production and water balance in desert-oasis region, northwest China.

Eddy covariance (EC) is recognized as the standard method to study energy, water vapor, and CO_2 exchange between the surface and atmosphere (Baldocchi, 2003). EC can accurately calculate evapotranspiration (ET) in boreal, temperate and tropical forests, grasslands, deserts, and agricultural ecosystems (Liu and Feng, 2012; Mccaughey et al., 1997; Yuan et al., 2014). Previous studies on energy and water vapor exchange in agricultural ecosystems have

* Corresponding author.
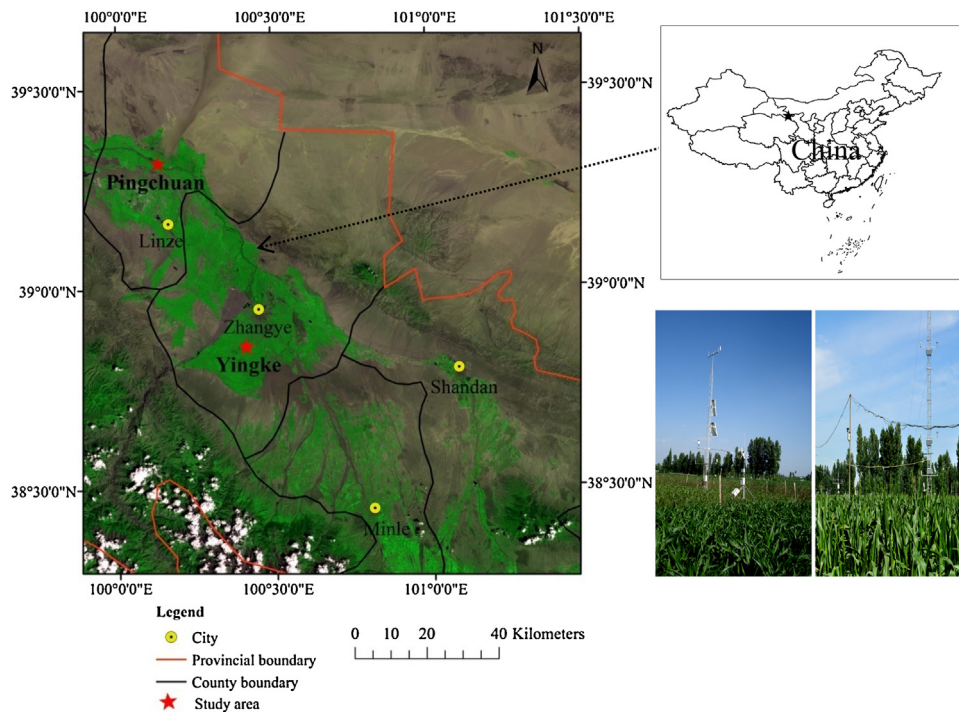E-mail address: zhangxyz23@126.com (Y. Zhang).

Fig. 1. Location of the two study areas—Yingke (a) and Pingchuan (b).

indicated considerable seasonal, interannual, and regional variation of energy budget and ET for different crop species (Ding et al., 2013; Steduto and Hsiao, 1998a,b; Suyker and Verma, 2008, 2009). Climate condition, vegetation growth, and soil moisture content are the main influential factors (Burba and Verma, 2005; Lei and Yang, 2010; Steduto and Hsiao, 1998b). The seasonal and interannual variability in evapotranspiration based on the long-term fluxes measurements is important for identifying climate, crop factors, and soil water which regulate fluxes at different temporal scales, and is important for developing exact irrigation scheduling and modeling crop production (Burba and Verma, 2005; Ding et al., 2013; Li et al., 2008). Quantitatively research how biotic and abiotic variables affect the energy budget and ET is needed in desert-oasis agroecosystems.

The desert-oasis agroecosystems is critical for food production in this area, and is prone to significant water shortages and drought. The oasis area of the Hexi Corridor in the middle reaches of the Heihe River has expanded since a water diversion scheme was implemented in 2000 (Zhang and Zhao, 2015a). Currently, 86% of the agricultural and domestic water supplied comes from the Heihe River, and 96% of that water is used for irrigation (Chen et al., 2003). Maize seed is one of the main food crops in the Hexi Corridor, northwestern China (Su et al., 2010). Extensive irrigation to ensure the quality of the maize seeds has lead to serious water shortage in recent years. Seed maize agrosystems in the Hexi Corridor have unique planting density, open canopy structure, low leaf area index, and discrepancy of water requirement in comparison to hybrid maize in other regions (Zhao, 2011; Zhao and Ji, 2010). Ground is mulched with plastic film to reduce soil evaporation in the field. To conserve and improve water use efficiency of maize, it is essential to accurately estimate ET and determine the controlling factors. ET comprises 60–80% of net radiation in a growing season in irrigated agrosystems (Suyker and Verma, 2008, 2009). Seasonal and long-term variations of ET are closely linked to ecosystem productivity, water dynamics, and regional climate change (Nemani et al., 2002; Suyker and Verma, 2009). However, fewer studies have

investigated seed maize ET with plastic mulch estimated by EC in desert-oasis region.

In this study, two similar irrigated seed maize fields with plastic mulch were measured by EC technique at Yingke and Pingchuan in 2009. The objectives of this study were to: (1) investigate seasonal variation in energy and water vapor fluxes in arid irrigated croplands; (2) examine the seasonal variability of ET; (3) quantify thresholds of variables that affect the magnitude of ET over desert-oasis agroecosystems.

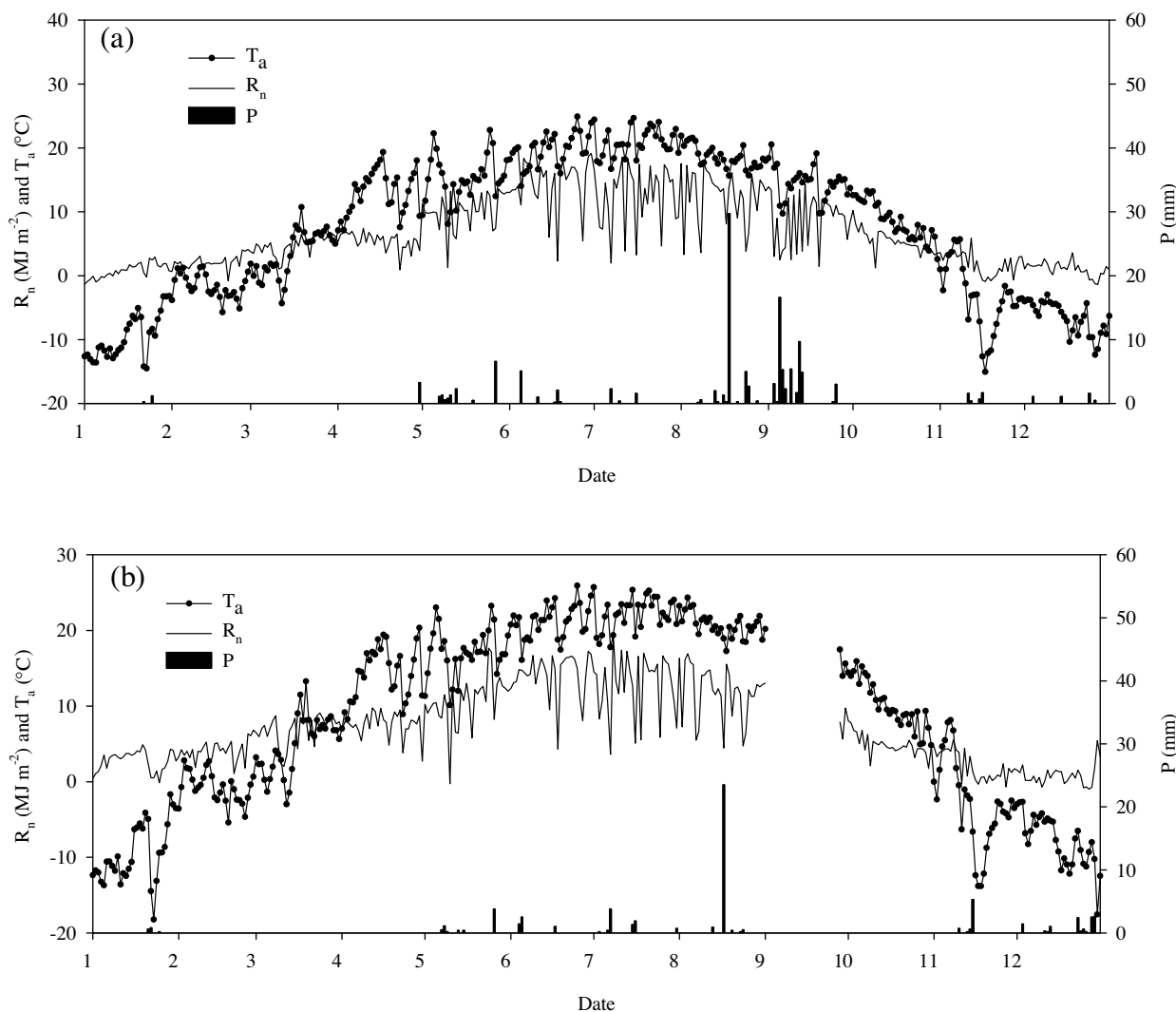## 2. Materials and methods

2.1. Study area

This study was conducted in a typical desert-oasis region in the middle reaches of the Heihe River Basin, located in the Hexi Corridor of Gansu Province (100°00′ E-100°30′ E, 38°50′ N-39°30′ N) (Fig. 1). The southern piedmont is an inclined oasis plain, and the northern is the margin of the Badain Jaran Desert. The major landscape types of this region are peripheral desert, desert-oasis ecotone, and central oasis. The study area has an arid climate characterized by cold winters and hot dry summers. The average annual temperature is 7.4 °C. The average annual precipitation is 124 mm with 70–80% occurring from May through September. The average annual pan evaporation is 2190 mm, which is twenty times greater than the annual precipitation. High winds and wind storms often occur in this area (Zhang and Zhao, 2015a,b). The soils are Anthrosols and some basic properties are summarized in Table 1.

In recent years, seed maize production has become the predominant agricultural crop in this desert-oasis region. Monoculture of spring maize with plastic mulching was planted for more than 10 years. Oasis croplands were sown with maize on April 10 and harvested on September 20. The rate of fertilizer application was approximately 300–450 kg^{-1} N ha^{-1}, 90–150 kg^{-1} P$_2$O$_5$ ha^{-1}, and 60–90 kg^{-1} K$_2$O ha^{-1} each year. During the growing season, maize was irrigated 4–7 times with more than 100 mm irrigating amount on each time depending on the soil conditions.

Table 1
Soil properties of study area.

Sites	Soil depth (cm)	Particle size distribution (%)			Texture classification	Bulk density (g cm^{-3})	Field capacity (cm^{-3} cm^{-3})	Soil organic carbon (g kg^{-1})
		Sand(0.05–2.00 mm)	Silt(0.002–0.05 mm)	Clay(<0.002 mm)				
Yingke	0–20	30.19	42.50	27.31	Loam	1.33	0.32	12.12
	20–40	27.79	46.77	25.44		1.38		
	40–100	32.53	43.80	23.68		1.46		
Pingchuan	0–20	63.68	31.71	4.61	Sandy loam	1.61	0.28	7.74
	20–40	58.49	36.95	4.56		1.59		
	40–100	56.81	38.54	4.65		1.59		

Fig. 2. Daily net radiation (R_n), air temperature (T_a), and precipitation (P) at Yingke (a) and Pingchuan (b) in 2009.

2.2. Energy flux and meteorological measurements

The study sites Yingke (100°24′ E, 38°51′ N, elevation 1519 m) and Pingchuan (100°08′ E, 39°19′ N, elevation 1381 m) were monitored in 2009. The Yingke observation site was established as part of the Heihe Watershed Allied Telemetry Experimental Research (HiWATER) project (Li et al., 2013). The Pingchuan observation site belongs to the Linze Inland River Basin Research Station, Chinese Ecosystem Research Network (Zhang and Zhao, 2015b). Both sites are large areas of uniform seed maize cropland.

EC technique was used to measure energy flux, H, and LE. A three-dimensional sonic anemometer (CSAT-3, Campbell Scientific Inc., Logan, UT, USA) with an open-path infrared H_2O/CO_2 gas analyzer (LI-7500, LI-COR Inc., Lincoln, NE, USA) was located 2.85 m above the maize canopy. The EC data were sampled at a frequency of 10 Hz by a data logger (Campbell Scientific, Inc., Logan, UT, USA), and then were processed with an average time of 30 min. An ENVIS Environmental Monitoring System (IMKO, Ettlingen, Germany) was mounted in the uniform croplands for long-term meteorological observations. Measurements of air temperature, relative humidity, air pressure, and wind speed and direction were made at 2 m and

10 m above ground level by using an HMP45C temperature probe and relative humidity probe (Vaisala, Finland), a PTB100 barometer probe (Vaisala), a LISA cup anemometer (Siggelkow GmbH, Germany), and a Young 8100 wind indicator (Siggelkow), respectively. A CNR-1 radiometers probe (Kipp & Zonen, Holand) was mounted 4 m above the canopy to measure radiation components. At the Yingke experimental site, soil temperature (Campbell-109, Campbell Scientific Instruments Inc.) and moisture (CS616, Campbell Scientific Instruments Inc.) were measured at 10, 20, 40, 80, 120, and 160 cm depths. Two heat flux plates (HFP01, Campbell Scientific Instruments Inc.) were buried at the depths of 5 cm and 15 cm, respectively. At the Pingchuan experimental site, soil temperature, at depths of 5, 10, 20, 40, 80, and 120 cm, and soil moisture, at depths of 10, 20, 50, 100, 200, and 300 cm, were measured with a Pt100 sensor (IMKO) and a time domain reflectometer TRIME-IT (IMKO), respectively. Three heat flux plates (HFP01, Campbell Scientific Instruments Inc.) were randomly buried at the depths of 5 cm. Precipitation was monitored with a RG50 tipping-bucket rainfall gauge (SEBA Hydrometrie GmbH, Gewerbestr, Germany). All parameters were measured every 30 min and recorded on data loggers.

All the EC data post processing was involved spike detection, time lag correction of H_2O/CO_2 relative to vertical wind components, frequency response correction, and coordinate rotation using planar fit method. A WPL (Webb–Pearman–Leuning) density correction was also applied to the flux calculations (Webb et al., 1980). The half-hourly turbulent flux and meteorological data were carefully controlled for quality and spurious data points caused by instrument malfunction, sensor maintenance, and bad weather were removed. EC data at the Yingke site from two long periods of time (September 5th to October 12th, and November 11st to December 11th) were missing due to equipment failure. Meteorological data at the Pingchuan site from September 2nd to September 28th were missing because of a power failure. The LE data gaps were filled using artificial neural network (ANN) and mean diurnal variations (MDV) methods (Falge et al., 2001; Zhang et al., 2014). The ANN method was applied when the synchronous meteorological data were available; otherwise, the MDV method was used. The gap-filling data were used only to analyze the seasonal variations in evapotranspiration (ET). The energy balance ratio was calculated as $\sum(H + LE)/\sum(R_n - G)$.

2.3. Parameter calculation and data analysis

Surface daily ET (mm day^{-1}) was calculated as follows:

$$ET = \frac{LE}{\lambda \rho_w} \tag{1}$$

where LE is the latent heat energy (MJ m^{-2} day^{-1}); λ is the latent heat of vaporization of water (2.45 kJ g^{-1}); ρ_w is water density (1 g cm^{-3}).

The daily reference evapotranspiration (ET$_0$) was calculated from Penman–Monteith equation corrected by FAO at daily scales (Allen et al., 1998).

$$ET_0 = \frac{0.408\Delta(R_n - G) + \gamma \frac{900}{T_a + 273}U(e_s - e_a)}{\Delta + \gamma(1 + 0.34U)} \tag{2}$$

where R_n is the net radiation (MJ m^{-2} day^{-1}), G is the soil heat flux (MJ m^{-2} day^{-1}), T_a is the air temperature at 2-m height ($^\circ$C), U is the wind speed at 2-m height (m s^{-1}), $e_s - e_a$ is the vapor pressure deficit (kPa), Δ is the slope of water vapor pressure curve (kPa $^\circ$C^{-1}), and γ is the psychrometric constant (kPa $^\circ$C^{-1}). The crop coefficient (K_c) is defined as the ratio of ET to ET$_0$.

We used canopy conductance (G_s) and the Priestley–Taylor coefficient α to interpret the seasonal variability in ET. To avoid the

occurrence of numerical instability, the midday data G_s were calculated by the midday average values (12:00–14:00) (Monteith and Unsworth, 1990):

$$G_s = \frac{\gamma LEg_a}{\Delta(R_n - G) + \rho_a c_p VPDg_a - LE(\Delta + \gamma)} \tag{3}$$

where LE is the latent heat flux (W m^{-2}), R_n the net radiation (W m^{-2}), G the soil heat flux (W m^{-2}), ρ_a is the air density (1.2 kg m^{-3}), c_p is the specific heat of the air (1004.7 J kg^{-1} $^\circ$C^{-1}), VPD is the vapor pressure deficit (kPa). Δ is the slope of water vapor pressure curve (kPa $^\circ$C^{-1}), and γ is the psychrometric constant (kPa $^\circ$C^{-1}). The aerodynamic conductance (g_a) was approximately estimated were calculated as follows (Monteith and Unsworth, 1990):

$$g_a = \left(\frac{U}{U_*^2} + 6.2U_*^{-2/3}\right)^{-1} \tag{4}$$

where U is the wind velocity (m s^{-1}), and U_* is the friction velocity estimated by the EC system. The Priestley–Taylor coefficient α is defined as the ratio of ET to the equilibrium evaporation (ET$_{eq}$), which was calculated as follows (Priestley and Taylor, 1972):

$$ET_{eq} = \frac{\Delta}{\Delta + \gamma}(R_n - G) \tag{5}$$

2.4. Path analysis

Path analysis was conducted to evaluate the direct and indirect effects of microclimate variables (R_n, T_a, VPD, and U) on ET and to determine the effectual meteorological variables. This method is more appropriate compared to multiple regression because the relationships between variables are either known or uncertain. The path analysis method is used not only to determine the relationship of variables but also to obtain the quantitative effect of the factors on the dependent variable. Path analysis depends on analyzing the direct effect of variables on the dependent variable and the indirect effect of variables on the dependent variable via other variables (See details in Zhang et al., 2012).

3. Results

3.1. Meteorological conditions and soil properties

The daily R_n, T_a, and precipitation (P) at Yingke and Pingchuan are shown in Fig. 2; and the seasonal variations of meteorological factors are shown in Tables 2 and 3. The climate in study area was relatively stable during the observation period, and displayed a parabolic trend. R_n, T_a, and VPD at both sites increased from winter to summer, with the highest values ($\sim$20 MJ m^{-2}, $\sim$25 $^\circ$C, and >2.0 kPa) during June–August (Figs. 2 and 3). The total P was 137.3 mm and 109.9 mm at Yingke and Pingchuan, respectively. The maximum wind speed (U) at Yingke and Pingchuan was 5.02 and 5.45 m s^{-1}, respectively, both occurring on Apirl 30th (Fig. 4). Wind speed gradually decreased with the increase of vegetation cover during June–September in this area. Both sites experienced similar microclimate conditions with cold winters and hot dry summers. Scarce precipitation, high solar radiation, and low air humidity are the main climatic features of the study area.

The soil is classified as loam and sandy loam at Yingke and Pingchuan, respectively (USDA classification system). The Yingke site had greater clay content (<0.002 mm), lower bulk density, and greater field capacity than the Pingchuan site (Table 1). In addition, soil organic carbon was greater at Yingke. Soil water content (SWC) in the maize root zone was significantly greater at Yingke than Pingchuan (Fig. 5, Tables 2 and 3). There were seven major fluctuations in soil moisture at Yingke (Fig. 5a) due to soil thawing

Table 2
Seasonal variations of major biometeorological factors at the Yingke site.

Month	Crop season	R_n (MJ m^{-2} day^{-1})	T_a (°C)	VPD (kPa)	U (m s^{-1})	ET (mm day^{-1})	ET$_0$ (mm day^{-1})	P (mm)	SWC (cm^3 cm^{-3})	T_s (°C)	LAI (m^2 m^{-2})	G_s (mm s^{-1})	α
1	Pre-growth	0.77	−9.67	0.13	1.40	0.31	0.41	1.5	0.12	−3.98	/	/	/
2		2.08	−1.63	0.32	1.74	0.33	1.05	0	0.13	−0.99	/	/	/
3		4.77	3.55	0.52	1.98	1.42	1.88	0	0.19	1.13	/	/	/
4	Spring	5.46	13.04	1.15	2.24	1.58	3.18	3.3	0.26	10.61	0.02	/	/
5	maize	10.14	15.24	1.04	1.97	2.38	3.84	14.6	0.24	16.46	0.20	2.25	0.46
6		14.45	19.72	1.25	1.44	4.08	4.99	8.7	0.29	20.39	1.70	4.16	0.70
7		12.51	20.91	1.07	1.16	4.67	4.32	4.6	0.29	20.26	4.00	7.30	0.90
8		12.59	18.56	0.78	0.99	3.89	3.97	42.9	0.29	17.19	3.63	5.34	0.76
9		8.73	14.53	0.50	0.97	2.51	2.64	52.6	0.32	14.56	1.53	/	/
10	Post-	5.38	8.64	0.57	1.49	1.47	2.06	0	0.25	9.91	/	/	/
11	harvest	1.90	−3.39	0.20	1.54	0.71	0.75	4.5	0.26	1.74	/	/	/
12		1.07	−6.59	0.13	1.51	0.45	0.48	4.6	0.19	−1.19	/	/	/

Mean net radiation (R_n), mean air temperature (T_a), mean vapor pressure deficit (VPD), mean wind speed (U), mean evapotranspiration (ET), mean reference evapotranspiration (ET$_0$), total precipitation (P), mean volumetric soil water content (0–80 cm averaged, SWC), mean soil temperature (0–10 cm averaged, T_s), mean leaf area index (LAI), mean midday canopy surface conductance (G_s), mean midday Priestley–Taylor coefficient (α), Midday was defined as 12:00 h through 14:00 h Beijing Standard Time (BST).

Table 3
Seasonal variations of major biometeorological factors at the Pingchuan site.

Month	Crop season	R_n (MJ m^{-2} day^{-1})	T_a (°C)	VPD (kPa)	U (m s^{-1})	ET (mm day^{-1})	ET$_0$ (mm day^{-1})	P (mm)	SWC (cm^3 cm^{-3})	T_s (°C)	LAI (m^2 m^{-2})	G_s (mm s^{-1})	α
1	Pre-growth	2.71	−9.61	0.12	1.41	0.14	0.67	1.7	0.16	−5.24	/	/	/
2		4.08	−0.84	0.35	1.78	0.25	1.34	0	0.15	−1.07	/	/	/
3		6.88	4.85	0.65	2.16	0.54	2.41	0	0.21	2.19	/	/	/
4	Spring	7.53	14.18	1.31	2.44	0.63	3.72	0	0.24	14.93	0.03	/	/
5	maize	10.70	17.13	1.33	2.20	1.59	4.17	6.4	0.25	19.58	0.24	1.41	0.36
6		14.18	21.27	1.44	1.20	4.08	4.53	5	0.26	21.84	2.27	5.09	0.89
7		12.90	22.22	1.11	0.70	4.39	4.15	8.3	0.27	20.20	3.83	8.28	1.00
8		11.88	20.75	1.00	0.82	3.63	3.82	25.6	0.27	19.06	3.10	5.21	0.77
9		/	/	/	/	1.53	/	44.1	/	/	1.66	/	/
10	Post-	4.90	10.20	0.74	1.44	0.68	2.12	0	0.26	12.48	/	/	/
11	harvest	2.08	−2.96	0.24	1.53	0.47	0.88	6.8	0.28	3.19	/	/	/
12		0.82	−7.93	0.10	1.57	0.22	0.48	12	0.23	−0.59	/	/	/

Mean net radiation (R_n), mean air temperature (T_a), mean vapor pressure deficit (VPD), mean wind speed (U), mean evapotranspiration (ET), mean reference evapotranspiration (ET$_0$), total precipitation (P), mean volumetric soil water content (0–100 cm averaged, SWC), mean soil temperature (0–10 cm averaged, T_s), mean leaf area index (LAI), mean midday canopy surface conductance (G_s), mean midday Priestley–Taylor coefficient (α), Midday was defined as 12:00 h through 14:00 h Beijing Standard Time (BST).
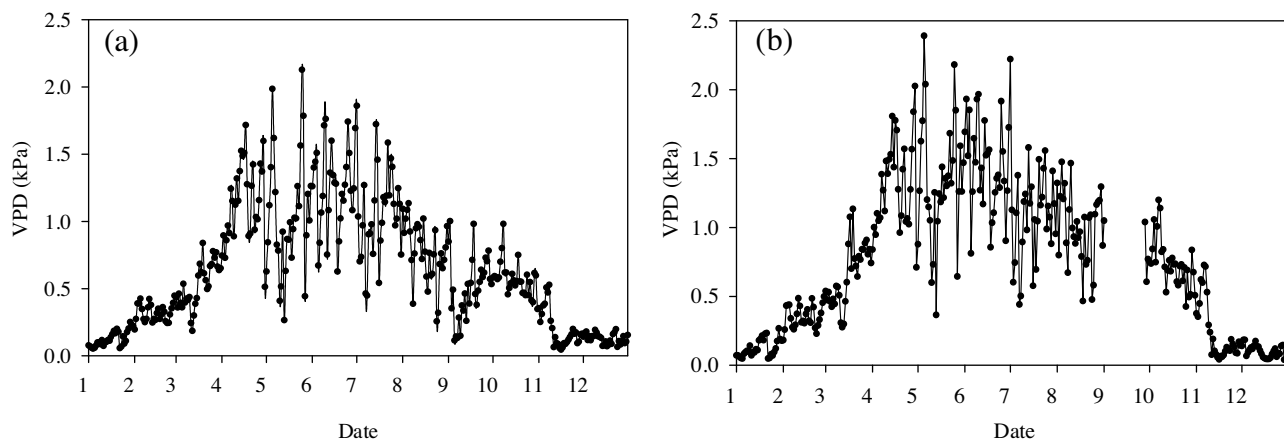

Fig. 3. Daily vapor pressure deficit (VPD) at Yingke (a) and Pingchuan (b) in 2009.

episodes in Apirl, five irrigation events, and one significant precipitation event on September 12th (Fig. 2a). There were nine major fluctuations in soil moisture at Pingchuan (Fig. 5b) due to soil thawing in Apirl, eight irrigation events (Fig. 2b). In early November, croplands were irrigated to maintain soil moisture content. The average 0–10 cm soil temperatures (T_s) at Yingke and Pingchuan were 8.32 and 9.69 °C, respectively. The maximum T_s occurred during June–August (Tables 2 and 3).

3.2. Surface energy balance and energy flux partitioning

The closure of surface energy balance was adopted to confirm the measurement accuracy of data. The regression statistics of the sum of sensible and latent fluxes (H + LE) on available energy flux (R_n-G) are shown in Table 4. Using half-hourly data, the slope between R_n-G and H + LE was 0.61 and 0.68, the intercept was 33.57 and 8.78 W m^{-2}, and the coefficient of determination (R^2) was 0.83 and 0.79 at Yingke and Pingchuan, respectively. The energy balance ratios were 0.99 and 0.79 at Yingke and Pingchuan, respectively.
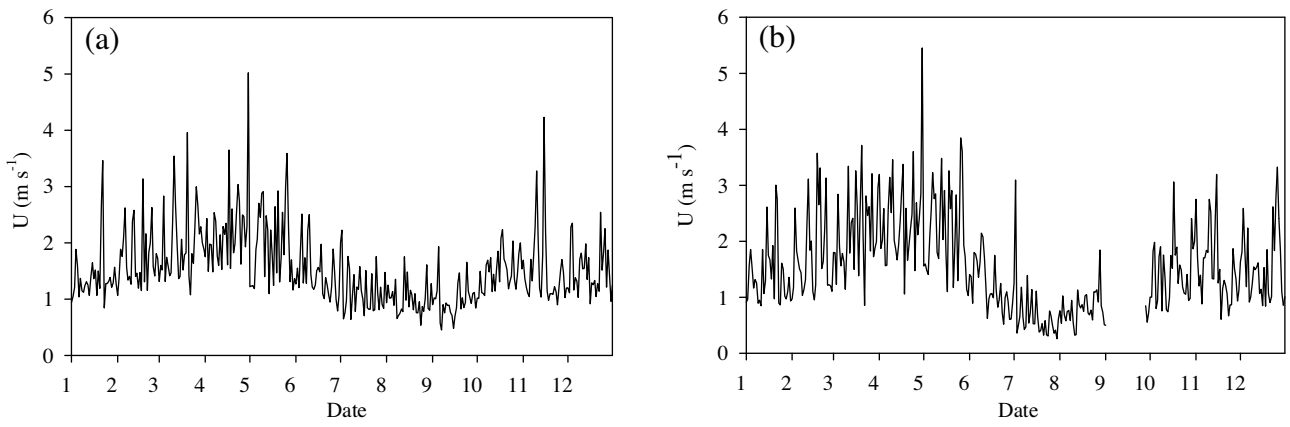
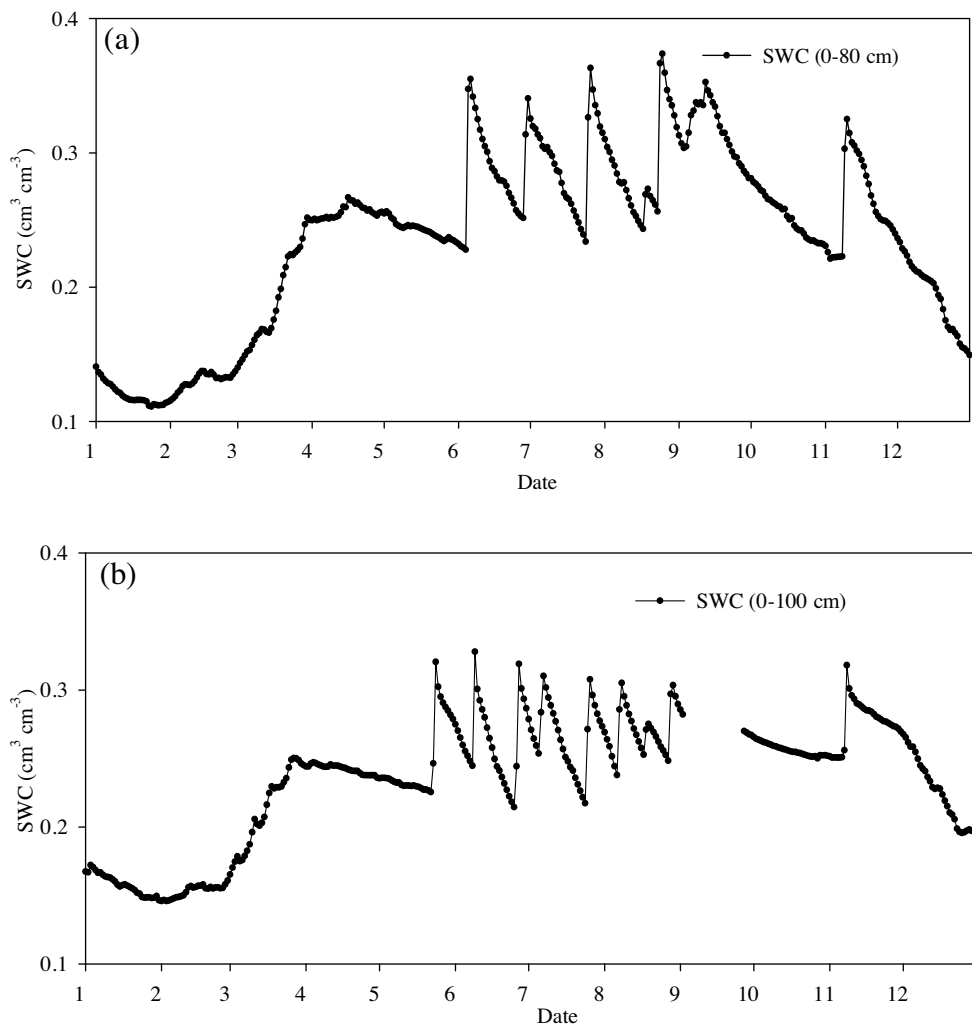**Fig. 4.** Daily wind speed (U) at Yingke (a) and Pingchuan (b) in 2009.

Fig. 5. Daily volumetric soil water content (SWC) at Yingke (a) and Pingchuan (b) in 2009.

Table 4
Linear regression coefficients for energy balance closure and the annual ratio of $\sum(H + LE)/\sum(R_n - G)$ in the two sites.

Site	Slope	Intercept (W m^{-2})	R^2	Data number	$\sum(H + LE)/\sum(R_n - G)$
Yingke	0.61	33.57	0.83	12266	0.99
Pingchuan	0.68	8.78	0.79	14344	0.79

Table 5
Average energy flux components of net radiation (R_n), sensible heat flux (H), and latent heat flux (LE), and the average energy partitions and average daily evapotranspiration (ET) in the two sites.

Site	Crop season	R_n(MJ m^{-2} day^{-1})	LE(MJ m^{-2} day^{-1})	H(MJ m^{-2} day^{-1})	ET(mm day^{-1})	LE/R_n	H/R_n
Yingke	Non-growth period	2.73	0.95	2.00	0.39	0.35	0.73
	Spring maize	11.15	8.20	2.61	3.35	0.74	0.23
Pingchuan	Non-growth period	3.58	0.94	2.95	0.38	0.26	0.82
	Spring maize	11.39	6.96	3.06	2.84	0.61	0.27
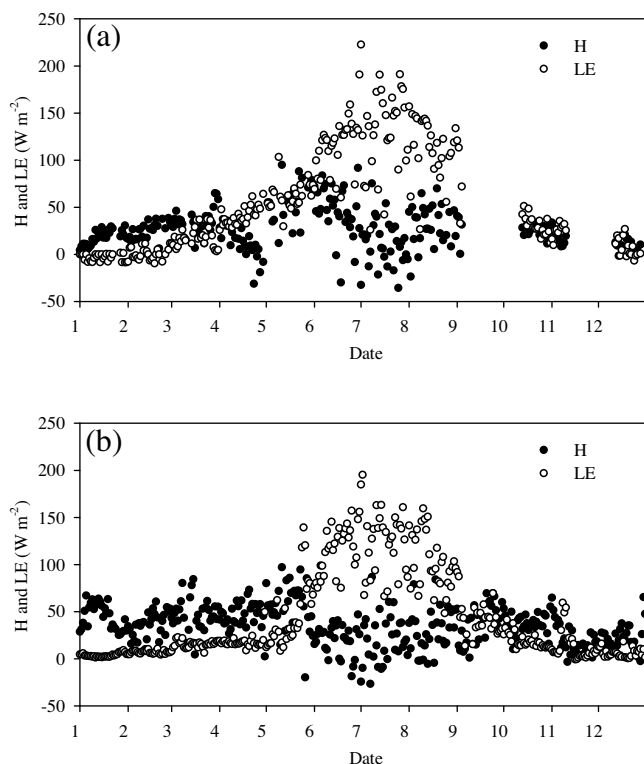
Fig. 6. Daily latent heat flux (LE) and sensible heat flux (H) at Yingke (a) and Pingchuan (b).

The average energy flux components in the growing season were much greater than that in the non-growing season although the duration was same (Table 5). In addition, the ratio of LE/R_n and H/R_n in the growing season at Yingke was 0.74 and 0.23; and the ratio of LE/R_n and H/R_n in the growing season at Pingchuan was 0.61 and 0.27. The latent heat flux was the main component in the growing season. The ratio of H/R_n was greater in the non-growing season than in the growing season. Therefore, R_n was mainly partitioned into LE and H. Net radiation was 11.27 MJ m^{-1} day^{-1} during the growing season. Latent heat flux accounted for 67.5% of net radiation, sensible heat flux was 25.0%, and soil heat flux was 7.5%.

The daily latent heat flux and sensible heat flux at Yingke and Pingchuan are shown in Fig. 6. The seasonal variations of LE and H were not consistent with R_n (Fig. 2). LE gradually increased over the growing season, but was near zero in the non-growing season. The daily H showed considerably smaller temporal variation. The daily H was negative in the growing season. The energy exchange was mainly in the form of latent heat flux in the growing season, whereas in the form of sensible heat flux in the non-growing season in oasis croplands.

3.3. Variation of ET

Leaf area index (LAI) during the growing season at Yingke and Pingchuan in 2009 was obtained from the reports of Wang et al.

(2013) and Zhao (2011). LAI increased with the growth of seed maize and reached the highest values (~4.0) in July (Table 2, Table 3, and Fig. 7). The male parent of seed maize was harvested in early August, producing a relatively open maize canopy.

In the non-growing season, the daily ET at Yingke and Pingchuan was less than 0.4 mm day^{-1} (Table 5). The seasonal variation in ET increased with ET$_0$, R_n, and T$_a$ (Tables 2 and 3). In the growing season, the variation of ET was similar to variations in LAI (Fig. 7). In both sites, ET generally reached peak values between 7.8 and 6.9 mm day^{-1} on July 1st (Fig. 7). The daily ET in the growing season was 3.35 and 2.84 mm day^{-1}, respectively (Table 5). In the entire growing season, ET was 545 and 467 mm in 2009, respectively. Fig. 8 shows the curvilinear relationship between maize K$_c$ and LAI from the seedling to maximum LAI. ET was significantly influenced by LAI below approximately 3.0 m^2 m^{-2}.

3.4. Abiotic and biotic variables

Path analysis was conducted to evaluate the direct and indirect effects of meteorological factors (R_n, T$_a$, VPD, and U) as independent variables on ET (Tables 6 and 7). At Yingke and Pingchuan, R_n and T$_a$ had the greater direct effect on ET among the independent variables. However, the greatest indirect effect of VPD on ET was mainly via R_n and T$_a$. R_n and T$_a$ had the greater direct effect and total effect on ET among the independent variables. Therefore, Variables R_n and T$_a$ in both sites were the major factors effect on maize ET.

The seasonal variation of midday G$_s$ (12:00–14:00) increased with increasing LAI (Tables 2 and 3). During the growing season, the maximum midday G$_s$ approached 14 mm s^{-1} (Fig. 9). The seasonal variation of Priestley–Taylor coefficient α was similar to variations in LAI and G$_s$ (Tables 2 and 3). There was a significantly positive relationship between G$_s$ and α in both sites (Fig. 9). The asymptotic values of α at Yingke and Pingchuan were 1.042 and 1.260, respectively. ET was significantly influenced by G$_s$ below approximately 10 mm s^{-1} (Fig. 9).

Irrigation appeared to increase ET on clear days, increasing by 1.27 mm day^{-1} at Yingke and 1.84 mm day^{-1} at Pingchuan (Fig. 10). ET decreased from 4.32 to 1.96 mm day^{-1} during the 4th irrigation at Yingke due to rainfall after application. ET decreased in the 2nd and 5th irrigation at Pingchuan resulting from cloudy and rainy days, respectively.

4. Discussion

4.1. Characteristics of energy flux partitioning over desert-oasis agroecosystems

To analyze the water vapor and energy exchange between agroecosystems and the atmosphere, it is necessary to understand the characteristics of energy flux partitioning. The energy balance closure statistics is usually used to evaluate the performance of the eddy-covariance system. In FLUXNET sites, Slope values range from 0.53 to 0.99 with a mean of 0.79, and intercept values range from −32.9 to 36.9 W m^{-2} with a mean of 3.7 W m^{-2} including grasslands, croplands, and forests (Wilson et al., 2002). In ChinaFLUX sites, Slope values range from 0.49 to 0.81 with a mean of 0.67,

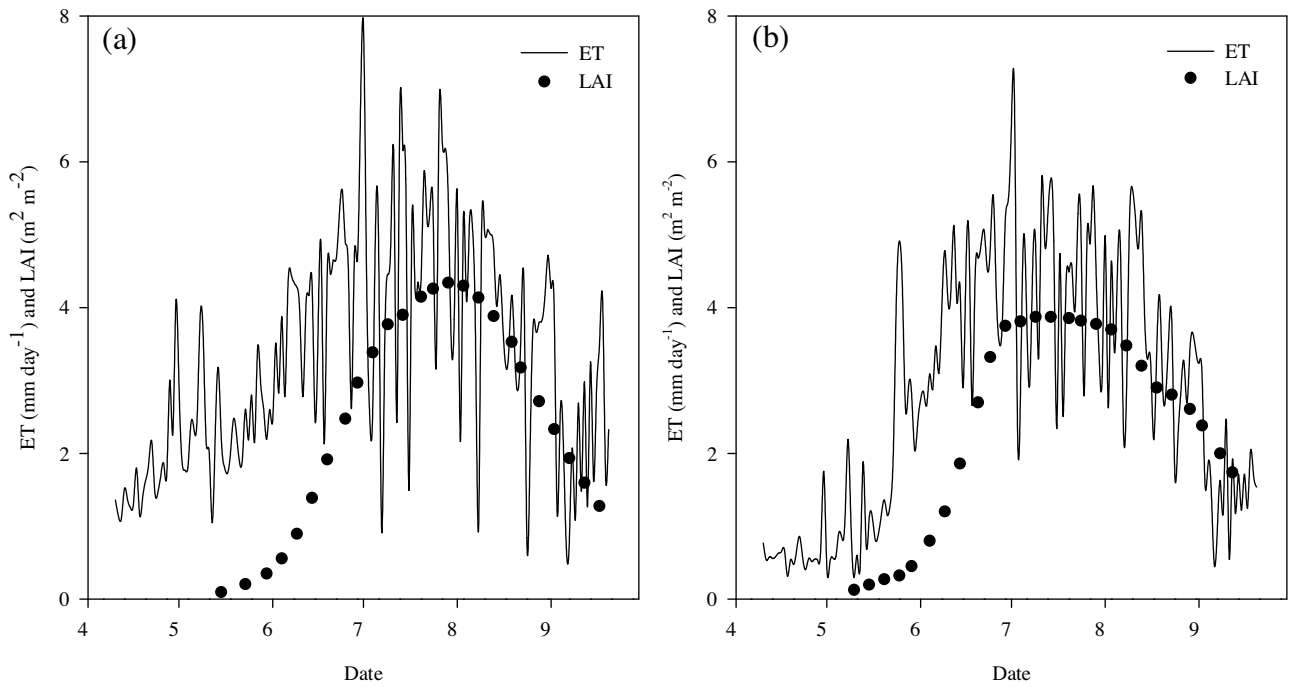**Fig. 7.** Daily evapotranspiration (ET) and LAI during maize growth stages at Yingke (a) and Pingchuan (b).
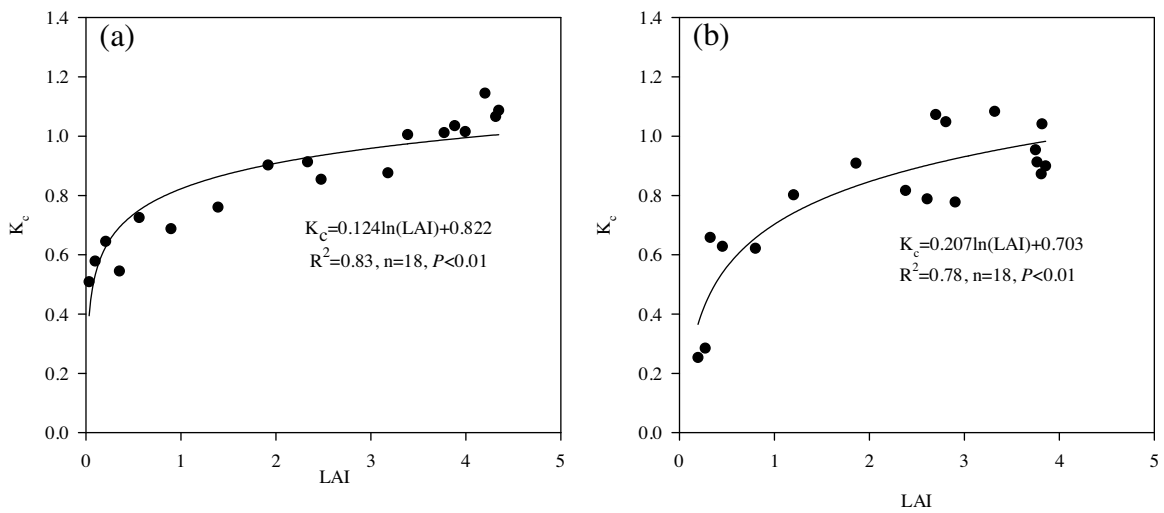

Fig. 8. Relations between LAI and K_c at Yingke (a) and Pingchuan (b). For this analysis, data are excluded on days when the canopy was senescing.

Table 6
Path analysis between ET and meteorological variables at the Yingke site.

Direct effect		Indirect effect via other independent variables		Indirect effect	Total effect
$R_n \to ET$	0.788	$R_n \to T_a \to ET$	0.163	0.122	0.910
		$R_n \to VPD \to ET$	−0.027		
		$R_n \to U \to ET$	−0.014		
$T_a \to ET$	0.195	$T_a \to VPD \to ET$	−0.032	0.619	0.814
		$T_a \to U \to ET$	−0.006		
		$T_a \to R_n \to ET$	0.657		
$VPD \to ET$	−0.038	$VPD \to U \to ET$	0.007	0.734	0.696
		$VPD \to R_n \to ET$	0.563		
		$VPD \to T_a \to ET$	0.164		
$U \to ET$	0.056	$U \to R_n \to ET$	−0.195	−0.222	−0.166
		$U \to T_a \to ET$	−0.022		
		$U \to VPD \to ET$	−0.005		

Net radiation (R_n), Air temperature (T_a), Vapor pressure deficit (VPD); Wind speed (U), Evapotranspiration (ET).
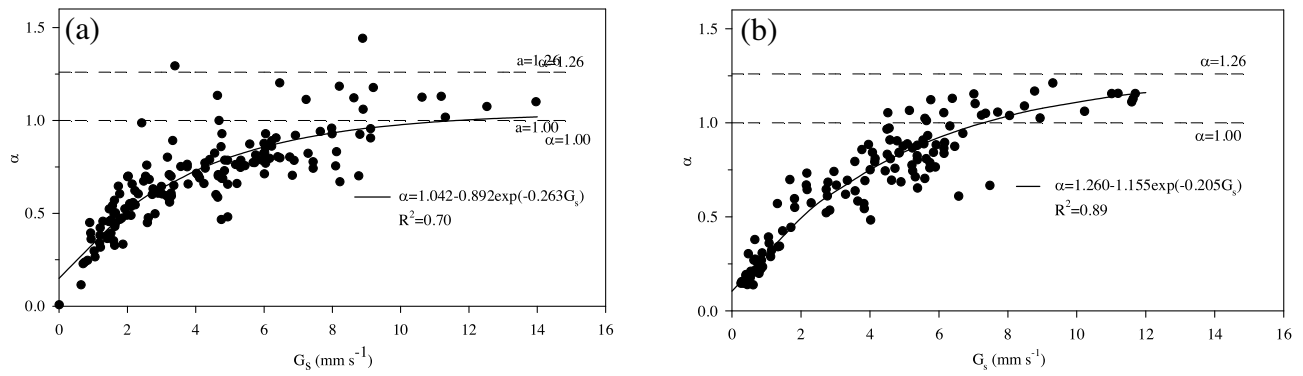
Fig. 9. Relations between mean midday canopy surface conductance (G_s) and mean midday Priestley–Taylor coefficient (α) at Yingke (a) and Pingchuan (b), $P < 0.05$, Midday was defined as 12:00 h through 14:00 h Beijing Standard Time (BST).
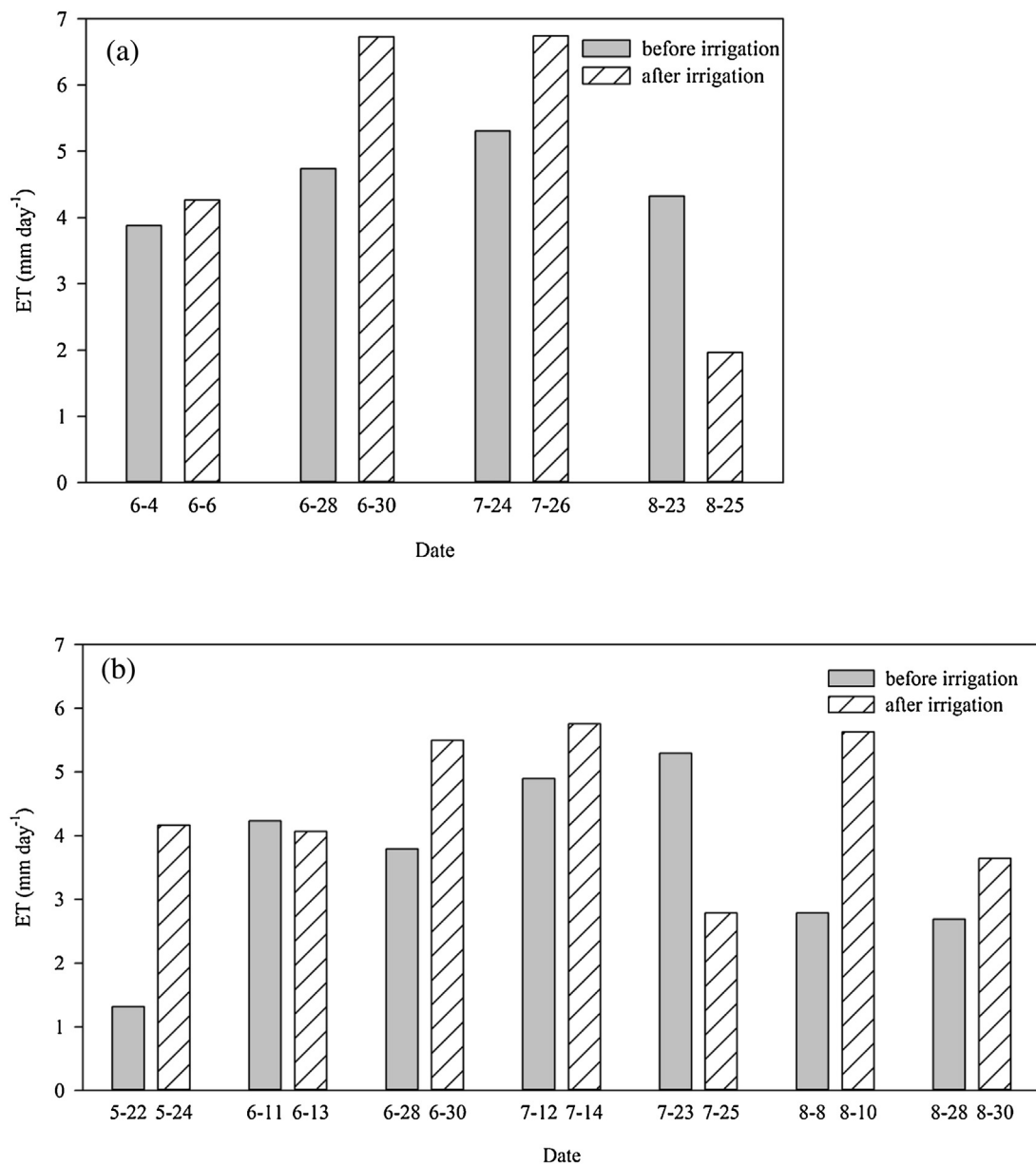

Fig. 10. Comparisons of ET before and after irrigation events at Yingke (a) and Pingchuan (b).

Table 7
Path analysis between ET and meteorological variables at the Pingchuan site.

Direct effect		Indirect effect via other independent variables		Indirect effect	Total effect
$R_n \to ET$	0.546	$R_n \to T_a \to ET$	0.345	0.255	0.801
		$R_n \to VPD \to ET$	−0.112		
		$R_n \to U \to ET$	0.022		
$T_a \to ET$	0.436	$T_a \to VPD \to ET$	−0.134	0.315	0.751
		$T_a \to U \to ET$	0.016		
		$T_a \to R_n \to ET$	0.432		
$VPD \to ET$	−0.159	$VPD \to U \to ET$	−0.002	0.750	0.591
		$VPD \to R_n \to ET$	0.385		
		$VPD \to T_a \to ET$	0.367		
$U \to ET$	−0.077	$U \to R_n \to ET$	−0.156	−0.251	−0.328
		$U \to T_a \to ET$	−0.091		
		$U \to VPD \to ET$	−0.004		

Net radiation (R_n), Air temperature (T_a), Vapor pressure deficit (VPD); Wind speed (U), Evapotranspiration (ET).

and intercept values range from 10.8 to 79.9 W m^{-2} with a mean of 28.9 W m^{-2} (Li et al., 2005). The average energy balance ratio in FLUXNET sites ranged from 0.34 to 1.69 with a mean of 0.84; and the ratio in ChinaFLUX sites ranged from 0.58 to 1.00 with a mean of 0.83 (Wilson et al., 2002; Li et al., 2005). The degree of energy balance closure in both sites were reasonable compared with the previous findings with different land use types, indicating that the EC measurements system provides reliable estimates of the surface energy balance components in desert-oasis agroecosystems.

The seasonal changes in R_n, LE, and H in both sites were similar, with very low values during the non-growing season, followed by a gradual increase in the growing season. The seasonal variation of LE was related to the phenology of maize. The daily H showed considerably smaller temporal variations. The seasonal variation in energy flux partitioning was significantly related to vegetation conditions (Table 5). During the growing season, the average LE/R_n was more than 60% for maize, which is comparable to an irrigated wheat-maize cropland in the North China Plain (57%, Lei and Yang, 2010). On an annual scale, the average LE/R_n was similar to a maize-soybean agroecosystem (Suyker and Verma, 2008, 2009) and an cultivated wheat ecosystems (Burba and Verma, 2005), but higher than a meadow ecosystem in the Qinghai–Tibetan Plateau (Gu et al., 2005), a typical steppe in Inner Mongolia (Hao et al., 2007), and a sub-alpine spruce forest ecosystem (Zhu et al., 2014). The latent heat flux was the largest consumer of net radiation during the growing season. There are opposite seasonal patterns of the H and LE fraction. In the non-growing season, the average H/R_n was more than 70% in both sites, which suggests the sensible heat flux was the largest consumer of net radiation from December to March in the bare field. Typically a few days following the first irrigation event in both sites, the sensible heat flux began to change direction and showed negative values for several days during the growing season (Fig. 6). This was likely the result of irrigation promoting sensible heat advection from the surrounding drier surface in the peripheral desert. The H was a source of energy due to the occurrence of sensible heat advection, particularly in the afternoon (Lei and Yang, 2010).

4.2. Characteristics of evapotranspiration over irrigated seed maize

Daily ET showed significant temporal variations in both sites related to the phenology of maize (Fig. 7). About 85% of annual ET occurred during the growing season from April to September in both sites. During the growing season, the total ET was 545 mm with a daily average value of 3.35 mm day^{-1} at Yingke, and the total ET was 467 mm with a daily average value of 2.84 mm day^{-1} at Pingchuan. Ding et al. (2013) observed a total ET of 503 and

562 mm, and mean daily ET 3.47 and 3.54 mm day^{-1} in an irrigated maize field with plastic mulch over two growing seasons in an arid region. The results of our study were comparable with that study site mainly due to similar EC technique. However, total ET was from 552 to 777 mm, and mean daily values from 3.73 to 5.26 mm day^{-1} in an irrigated maize field in the middle Heihe River basin, China (Zhao et al., 2010), which is greater than our results. The reason is that Zhao et al. (2010) estimated total ET by using the soil water balance and Bowen ratio-energy balance methods. The results in our study sites were greater than total ET of irrigated maize in semi-humid regions in China (Kang et al., 2003; Liu et al., 2010b; Zhang et al., 2011). Differences in ET over irrigated maize fields are mainly caused by climate conditions, measurement method, and mulching pattern.

During the growing season, daily ET generally reached peak values in a sunny day, comparable to other irrigated croplands (Howell et al., 1998; Kjelgaard and Stockle, 2001). From post-harvest to the middle of April, ET showed considerably smaller temporal variation. Daily ET was mainly to the result of soil evaporation because the maize transpiration would not have occurred. During this period, daily ET was generally less than 0.4 mm day^{-1}, which was limited by a few factors, such as solar radiation, temperature, and soil freezing episodes (Wever et al., 2002).

4.3. The meteorological factors, biological factors, and irrigation controlling ET

The magnitude of ET is considered to be a multivariate phenomenon as it is influenced by meteorological variables (Ding et al., 2013; Hao et al., 2007). Our results revealed that R_n and T_a in both sites were the major meteorological variables affecting the seasonal variability of daily ET. Law et al. (2002) and Li et al. (2008) reported that R_n is the major driving factor of ET, which is in agreement with our results. These results confirm that radiation energy or available energy is the critical factor for controlling the seasonal variability of daily ET over seed maize agroecosystems in desert-oasis region.

Vegetation, especially LAI, has a significant impact on ET (Li et al., 2008; Steduto and Hsiao, 1998b). The highest value of seed maize LAI (~4.0) is less than hybrid maize LAI with the highest value (~6.0) (Ding et al., 2013; Liu et al., 2010b; Steduto and Hsiao, 1998b; Suyker and Verma, 2008). Maize LAI decrease when water is limited during the seedling stage (Allen et al., 1998; Ding et al., 2013), which results in a slow increase in ET (Fig. 7). An increase in LAI will increase K_c from the seedling to heading stages when soil relative extractable water is more than 0.5 (Burba and Verma, 2005; Lei and Yang, 2010). This response weakens at maximum LAI when the crop transpires at near-potential rates. The K_c in our study sites increased with an increase of LAI until the threshold LAI,

generally seed maize LAI of 3.0 m² m⁻² (Fig. 8). This is similar to results of Suyker and Verma (2008) who found a nearly linear relationship between the daily K_c and LAI until a threshold LAI around 3–4 m² m⁻² was reached. Steduto and Hsiao (1998b) suggested a slightly higher threshold of 4.5 m² m⁻². The results suggest that ET is significantly affected by LAI below a certain threshold.

The Priestley–Taylor coefficient α helps diagnose how biotic factors control daily ET relative to the amount of available energy (Arain et al., 2003). The daily α were rarely less than 0.5 during the growing season (Tables 2 and 3), which reflects the very limited control of soil moisture on ET in both sites (Liu et al., 2010a). Canopy conductance was explored to provide seasonal information on the biosphere's control of ET (Baldocchi et al., 2004; Schulze et al., 1994). Higher ET is often associated with greater G_s, although the effect of G_s and environment conditions on ET varies widely among vegetation types and environmental conditions (Liu et al., 2010a; Wever et al., 2002; Zhu et al., 2014). The G_s values in both sites were lower than that in relatively closed maize canopy (Steduto and Hsiao 1998b; Suyker and Verma, 2008), which is due to the harvesting of the male parent of corn. The significantly positive relationships between G_s and α suggested that ET is greatly influenced by canopy conductance (Fig. 9). The Priestley–Taylor coefficient significantly increased with increasing G_s when $G_s \leq 10$ mm s⁻¹ and almost remained constant when $G_s > 10$ mm s⁻¹. A theoretical study on a fully developed canopy indicates that ET is insensitive to canopy conductance when $G_s > 16$ mm s⁻¹ (Ding et al., 2013; Lei and Yang, 2010; McNaughton and Spriggs, 1986). The threshold G_s values (≤ 10 mm s⁻¹) in our study sites were lower than previous results possibly due to the open seed maize canopy.

In arid and semi-arid regions, irrigation often strongly influences the surface energy exchange and ET over agroecosystems. The daily α values are significantly correlated with soil relative extractable water (Baldocchi et al., 2004; Liu et al., 2010a). Moreover, ET is greatly influenced by soil water storage when the soil relative extractable water values are below a threshold value (Burba and Verma, 2005; Ding et al., 2013; Lei and Yang, 2010). The sensible heat advection caused by regional irrigation enhances evapotranspiration further affecting the local energy budget (Lei and Yang, 2010). The sensible heat flux is higher, the latent heat flux is lower, and the Bowen ratio increases without the ample water in an oasis. Oases will gradually degenerate into desert without irrigation (Gao et al., 2002). Therefore, water is crucial in oases and irrigation maintains the development of oasis agroecosystems. Regional irrigation in Irrigation District has shifted the pattern of annual water-energy balance and total ET in desert-oasis region.

5. Conclusions

Using the eddy covariance technique, water vapor and energy fluxes were measured for irrigated seed maize fields in desert-oasis agroecosystems in 2009. The climate in study area was relatively stable during the observation period, and displayed a parabolic dynamic. The slope between R_n-G and H + LE were 0.61 and 0.68, the intercept was 33.57 and 8.78 W m⁻², and the coefficient of determination (R^2) were 0.83 and 0.79 in both sites for half-hourly time scale, respectively. The energy balance closure statistics suggested adequate performance of the eddy covariance systems at our sites. The seasonal changes in net radiation (R_n), latent heat flux (LE), and sensible heat flux (H) were similar between the two study sites, with very low values during the non-growing season, followed by a gradual increase in the growing season. The seasonal variation of LE was strongly related to the phenology of the maize. The daily H showed less temporal variation. In desrt-oasis agroecosystems, maize transpiration occupies most of the surface ET, which causes

the unique seasonal processes of energy flux partitioning in the study area. The average LE/R_n was more than 60% during the growing season, the average H/R_n was more than 70% for both sites in the non-growing season.

The daily ET showed significantly temporal variation in both sites. ET ranged 467–545 mm for maize with the daily ET 2.84–3.35 mm day⁻¹. The daily ET was mainly controlled by net radiation and air temperature, and was significantly influenced by LAI (≤ 3.0 m² m⁻²), canopy conductance (≤ 10 mm s⁻¹). Moreover, regional irrigation in Irrigation District strongly influences the pattern of annual water-energy balance and total ET in desert-oasis region, northwest China.

References

Allen, R.G., Pereira, L.S., Reas, D., Smith, M., 1998. Guidelines for Computing CropWater Requirements, FAO Irrigation and Drainage Paper No. 56. United Nations, FAO, Roma, Italy.

Arain, M.A., Black, T.A., Barr, A.G., Griffis, T.J., Morgenstern, K., Nesic, Z., 2003. Year round observations of the energy water vapor fluxes above a boreal black spruce forest. Hydrol. Process. 17, 3581–3600.

Baldocchi, D., Kelliher, F.M., Black, T.A., Jarvis, P., 2000. Climate and vegetation controls on boreal zone energy exchange. Glob. Change Biol. 6 (suppl 1), 69–83.

Baldocchi, D.D., Xu, L.K., Kiang, N., 2004. How plant functional-type, weather, seasonal drought, and soil physical properties alter water and energy fluxes of an oak-grass savanna and an annual grassland. Agric. For. Meteorol. 123, 13–39.

Baldocchi, D.D., 2003. Assessing the eddy covariance technique for evaluating carbon dioxide exchange rates of ecosystems: past, present and future. Glob. Change Biol. 9, 479–492.

Burba, G.G., Verma, S.B., 2005. Seasonal and interannual variability in evapotranspiration of native tallgrass prairie and cultivated wheat ecosystems. Agric. For. Meteorol. 135 (1), 190–201.

Chen, D.J., Xu, Z.M., Chen, R.S., 2003. Design of resources accounts: a case of integrated environmental and economic accounting. Adv. Water Sci. 14, 631–637 (in Chinese with English abstract).

Chen, S.P., Chen, J.Q., Lin, G.H., Zhang, W.L., Miao, H.X., Wei, L., Huang, J.H., Han, X.G., 2009. Energy balance and partition in Inner Mongolia steppe ecosystems with different land use types. Agric. For. Meteorol. 149 (11), 1800–1809.

Ding, R.S., Kang, S.Z., Li, F.S., Zhang, Y.Q., Tong, L., 2013. Evapotranspiration measurement and estimation using modified Priestley–Taylor model in an irrigated maize field with mulching. Agric. For. Meteorol. 168, 140–148.

Falge, E., Baldocchi, D.D., Olson, R., et al., 2001. Gap filling strategies for defensible annual sums of net ecosystem exchange. Agric. For. Meteorol. 107, 43–69.

Gao, Y.H., Chen, Y.C., Lv, S.H., 2002. Role of irrigation in maintenance and development of modern oasis. J. Desert Res. 22 (4), 383–386 (in Chinese with English abstract).

Gu, S., Tang, Y.H., Cui, X.Y., Kato, T., Du, M.Y., Li, Y.N., Zhao, X.Q., 2005. Energy exchange between the atmosphere and a meadow ecosystem on the Qinghai–Tibetan Plateau. Agric. For. Meteorol. 129 (3), 175–185.

Hao, Y.B., Wang, Y.F., Huang, X.Z., Cui, X.Y., Zhou, X.Q., Wang, S.P., Niu, H.S., Jiang, G.M., 2007. Seasonal and interannual variation in water vapor and energy exchange over a typical steppe in Inner Mongolia, China. Agric. For. Meteorol. 146 (1), 57–69.

Howell, T.A., Tolk, J.A., Schneider, A.D., Evett, S.R., 1998. Evapotranspiration, yield, and water use efficiency of corn hybrids differing in maturity. Agron. J. 90, 3–9.

Kang, S.Z., Gu, B.J., Du, T.S., Zhang, J.H., 2003. Crop coefficient and ratio of transpiration to evapotranspiration of winter wheat and maize in a semi-humid region. Agric. Water Manage. 59 (3), 239–254.

Kjelgaard, J.F., Stockle, C.O., 2001. Evaluating surface resistance for estimating corn and potato evapotranspiration with the Penman–Monteith model. Trans. ASAE 44 (4), 797–805.

Law, B.E., Falge, E., Gu, L., et al., 2002. Environmental controls over carbon dioxide and water vapor exchange of terrestrial vegetation. Agric. For. Meteorol. 113, 97–120.

Lei, H.M., Yang, D.W., 2010. Interannual and seasonal variability in evapotranspiration and energy partitioning over an irrigated cropland in the North China Plain. Agric. For. Meteorol. 150 (4), 581–589.

Li, Z.Q., Yu, G.R., Wen, X.F., Zhang, L.M., Ren, C.Y., Fu, Y.L., 2005. Energy balance closure at ChinaFLUX sites. Sci. China Ser. D-Earth Sci. 48 (suppl), 51–62.

Li, S.E., Kang, S.Z., Li, F.S., Zhang, L., 2008. Evapotranspiration and crop coefficient of spring maize with plastic mulch using eddy covariance in northwest China. Agric. For. Meteorol. 95 (11), 1214–1222.

Li, X., Cheng, G.D., Liu, S.M., et al., 2013. Heihe watershed allied telemetry experimental research (HiWATER): Scientific objectives and experimental design. Bull. Am. Meteorol. Soc. 94 (8), 1145–1160.

Liu, H.Z., Feng, J.W., 2012. Seasonal and interannual variations of evapotranspiration and energy exchange over different land surfaces in a semiarid area of China. J. Appl. Meteorol Climatol. 51 (10), 1875–1888.

Liu, S., Li, S.G., Yu, G.R., Asanuma, J., Sugita, M., Zhang, L.M., Hu, Z.M., Wei, Y.F., 2010a. Seasonal and interannual variations in water vapor exchange and surface water balance over a grazed steppe in central Mongolia. Agric. Water Manage. 97 (6), 857–864.

Liu, Y., Yang, S.J., Li, S.Q., Chen, X.P., Fang, C., 2010b. Growth and development of maize (Zea mays L.) in response to different field water management practices: resource capture and use efficiency. Agric. For. Meteorol. 150 (4), 606–613.

McNaughton, K.G., Spriggs, T.W., 1986. A mixed-layer model for regional evaporation. Bound. Layer Meteorol. 34 (3), 243–262.

Mccaughey, J.H., Lafleur, P.M., Joiner, D.W., Bartlett, P.A., Costello, A.W., Jelinski, D.E., Ryan, M.G., 1997. Magnitudes and seasonal patterns of energy, water, and carbon exchanges at a boreal young jack pine forest in the BOREAS northern study area. J. Geophys. Res. 102 (D24), 28997–29007.

Monteith, J.L., Unsworth, M.H., 1990. Principles of Environmental Physics, 2nd ed. Chapman & Hall, New York, USA.

Nemani, R., White, M., Thornton, P., Nishida, K., Reddy, S., Jenkins, J., Running, S., 2002. Recent trends in hydrologic balance have enhanced the terrestrial carbon sink in the United States. Geophys. Res Lett. 29 (10), 106–111.

Priestley, C.H.B., Taylor, R.J., 1972. On the assessment of surface heat flux and evaporation using large-scale parameters. Mon. Weather Rev. 100, 81–92.

Schulze, E.D., Kelliher, F.M., Korner, C., Lloyd, J., Leuning, R., 1994. Relationships among maximum stomatal conductance, ecosystem surface conductance, carbon assimilation rate, and plant nutrition: a global scaling exercise. Ann. Rev. Ecol. Syst. 25, 629–660.

Sen, Z., 2004. Solar energy in progress and future research trends. Prog. Energy Combust. Sci. 30 (4), 367–416.

Steduto, P., Hsiao, T.C., 1998a. Maize canopies under two soil water regimes: I. Diurnal patterns of energy balance, carbon dioxide flux, and canopy conductance. Agric. For. Meteorol. 89 (3), 169–184.

Steduto, P., Hsiao, T.C., 1998b. Maize canopies under two soil water regimes: II. Seasonal trends of evapotranspiration, carbon dioxide assimilation and canopy conductance, and as related to leaf area index. Agric. For. Meteorol. 89 (3), 185–200.

Su, Y.Z., Yang, R., Liu, W.J., Wang, X.F., 2010. Evolution of soil structure and fertility after conversion of native sandy desert soil to irrigated cropland in arid region, China. Soil Sci. 175 (5), 246–254.

Suyker, A.E., Verma, S.B., 2008. Interannual water vapor and energy exchange in an irrigated maize-based agroecosystem. Agric. For. Meteorol. 148 (3), 417–427.

Suyker, A.E., Verma, S.B., 2009. Evapotranspiration of irrigated and rainfed maize–soybean cropping systems. Agric. For. Meteorol. 149 (3), 443–452.

Wang, J., Li, X., Lu, L., Fang, F., 2013. Estimating near future regional corn yields by integrating multi-source observations into a crop growth model. Eur. J. Agron. 49, 126–140.

Webb, E.K., Pearman, G.I., Leuning, R., 1980. Correction of the flux measurements for density effects due to heat and water vapour transfer. Quart. J. Roy. Meteorol. Soc. 106, 85–100.

Wever, L.A., Flanagan, L.B., Carlson, P.J., 2002. Seasonal and interannual variation in evapotranspiration, energy balance and surface conductance in northern temperate grassland. Agric. For. Meteorol. 112 (1), 31–49.

Wilson, K., Goldstein, A., Falge, E., et al., 2002. Energy balance closure at FLUXNET sites. Agric. For. Meteorol. 113 (1), 223–243.

Yuan, G.F., Zhang, P., Shao, M.A., Luo, Y., Zhu, X.C., 2014. Energy and water exchanges over a riparian Tamarix spp. stand in the lower Tarim River basin under a hyper-arid climate. Agric. For. Meteorol. 194, 144–154.

Zhang, Y.Y., Zhao, W.Z., 2015a. Effects of variability in land surface characteristics on the summer radiation budget across desert-oasis region in Northwestern China. Theor. Appl. Climatol. 119 (3-4), 771–780.

Zhang, Y.Y., Zhao, W.Z., 2015b. Vegetation and soil property response of short-time fencing in temperate desert of the Hexi Corridor northwestern China. Catena 133, 43–51.

Zhang, X., Chen, S., Sun, H., Shao, L., Wang, Y., 2011. Changes in evapotranspiration over irrigated winter wheat and maize in North China Plain over three decades. Agric. Water Manage. 98 (6), 1097–1104.

Zhang, Y.Y., Wu, P.T., Zhao, X.N., Li, P., 2012. Evaluation and modelling of furrow infiltration for uncropped ridge–furrow tillage in Loess Plateau soils. Soil Res. 50 (5), 360–370.

Zhang, K., Zhu, G.F., Bai, Y., Ma, T., 2014. Gap filling for evapotranspiration based on BP artificial neural networks. J. Lanzhou Univ. 53 (3), 348–355 (in Chinese with English abstract).

Zhao, L.W., Ji, X.B., 2010. Quantification of transpiration and evaporation over agricultural field using the FAO-56 dual crop coefficient approach—a case study of the maize field in an oasis in the middlestream of the Heihe River Basin in Northwest China. Sci. Agric. Sin. 43 (19), 4016–4026 (in Chinese with English abstract).

Zhao, W.Z., Liu, B., Zhang, Z.H., 2010. Water requirements of maize in the middle Heihe River Basin, China. Agric. Water Manage. 97 (2), 215–223.

Zhao, L.W., 2011. Observation and simulation of evapotranspiration over the maize field within an artifical oasis in the middlestream of Heihe River basin, Northwest China. In: Ph.D. Thesis. Chinese academy of sciences, China (in Chinese with English abstract).

Zhu, G.F., Lu, L., Su, Y.H., Wang, X.F., Cui, X., Ma, J.Z., He, J.H., Zhang, K., Li, C.B., 2014. Energy flux partitioning and evapotranspiration in a sub-alpine spruce forest ecosystem. Hydrol. Process. 28 (19), 5093–5104.